The Journal of Experimental Biology 214, 1369-1378

doi:10.1242/jeb.051136

RESEARCH ARTICLE

Slipping, sliding and stability: locomotor strategies for overcoming low-friction surfaces

Andrew J. Clark*,† and Timothy E. Higham

Department of Biological Sciences, Clemson University, 132 Long Hall, Clemson, SC 29634, USA

*Present address: Department of Biology, College of Charleston, 58 Coming Street, Room 214, Charleston, SC 29401, USA
†Author for correspondence (clarkaj@cofc.edu)

Accepted 7 January 2011

SUMMARY

Legged terrestrial animals must avoid falling while negotiating unexpected perturbations inherent to their structurally complex environments. Among humans, fatal and nonfatal injuries frequently result from slip-induced falls precipitated by sudden unexpected encounters with low-friction surfaces. Although studies using walking human models have identified some causes of falls and mechanisms underlying slip prevention, it is unclear whether these apply to various locomotor speeds and other species. We used high-speed video and inverse dynamics to investigate the locomotor biomechanics of helmeted guinea fowl traversing slippery surfaces at variable running speeds (1.3–3.6 m s^{-1}). Falls were circumvented when limb contact angles exceeded 70 deg, though lower angles were tolerated at faster running speeds (>3.0 m s^{-1}). These prerequisites permitted a forward shift of the body's center of mass over the limb's base of support, which kept slip distances below 10 cm (the threshold distance for falls) and maximized the vertical ground reaction forces, thus facilitating limb retraction and the conclusion of the stance phase. These postural control strategies for slip avoidance parallel those in humans, demonstrating the applicability of these strategies across locomotor gaits and the potential for guinea fowl as an insightful model for invasive approaches to understanding limb neuromuscular control on slippery surfaces.

Supplementary material available online at http://jeb.biologists.org/cgi/content/full/214/8/1369/DC1

Key words: running, perturbation, slipping, guinea fowl, injury.

INTRODUCTION

Limbed terrestrial animals routinely traverse highly variable terrain in three-dimensionally complex environments and the underlying mechanisms by which these tasks are negotiated bear strong ecological, evolutionary and biomedical implications. Whether it is an arboreal animal encountering a network of branches or a human encountering a patch of ice, animals must maintain adequate limb control to avoid falling. Terrestrial animals encompass a remarkable diversity in morphology and body size (Cavagna et al., 1977), and several studies have highlighted their ability to adapt to unpredictable terrain *via* behavioral and functional strategies (e.g. Daley et al., 2006). For example, lizard forelimbs and hindlimbs undergo substantial kinematic decoupling when traversing obstacles and utilize various behavioral strategies when negotiating exceptionally large obstacles (Kohlsdorf and Biewener, 2006). In addition, the supporting limbs of helmeted guinea fowl, when experiencing a sudden drop in terrain height, maintain dynamic stability by performing either net negative or positive work, depending on conditions at limb contact (Daley and Biewener, 2006; Daley et al., 2007). Dynamic stability is achieved when a fall is avoided and steady periodic movements of the center of mass (COM) relative to the base of support (BOS) are restored after a perturbation is experienced (Full et al., 2002; Daley et al., 2006). Determining how animals can respond quickly to unexpected changes in habitat structure will ultimately yield important information regarding the flexibility of physiological and behavioral systems.

Perturbation experiments are informative approaches to understanding the neuromechanical pathways to achieving dynamic stability and avoiding falls in realistic unsteady conditions (Biewener and Daley, 2007; Nishikawa et al., 2007). Control strategies have been demonstrated in terrestrial animals experiencing unexpected forces (Jindrich and Full, 2002), changes in substrate height (Daley and Biewener, 2006; Sponberg and Full, 2008) and altered ground compliance (Ferris et al., 1999). When experiencing erratic mechanical energy patterns introduced by perturbations, the supporting limb must produce, absorb, store-and-release and/or convert energy to achieve stability (Biewener and Gillis, 1999; Daley et al., 2006; Sponberg and Full, 2008). These responses are mediated by feedforward control, feedback control and intrinsic properties of the musculoskeletal system (Daley et al., 2007; Sponberg and Full, 2008).

An important perturbation that an animal could encounter is a sudden decrease in surface roughness and thus a change in the frictional force between the supporting limb and the ground. Traversing low-friction surfaces presents a major problem: failure to achieve minimum required coefficients of friction, which results in slipping (inability to maintain limb contact stability) (Cooper et al., 2008). Among humans, slips are a significant cause of falls, which can result in injury, disability and death, all of which increase in likelihood with age (Tinetti and Williams, 1997; Kannus et al., 2005). Furthermore, slips account for ~44% of fatal and nonfatal occupational falls (US Bureau of Labor Statistics, 1992; SWEA and Statistics Sweden, 2000). The biomechanics of slipping has previously been examined in human (e.g. Strandberg and Lanshammar, 1981; Cham and Redfern, 2001; Moyer et al., 2006) and animal models (Phillips and Morris, 2001; Thorup et al., 2008).

Despite the prevalence of slipping research and its broader significance in elucidating human postural control strategies to avoiding falls, our knowledge is restricted to walking subjects. Thus, it is unclear how falls can be avoided while running.

Moving at variable speeds is a vital characteristic of natural unsteady locomotion. Structurally complex environments necessitate diverse locomotor behaviors (acceleration, turns, stops, etc.), which require changes in speed (e.g. Higham et al., 2001). At a given moment during travel, a terrestrial animal must use a particular gait, such as walking or running. Gait characteristics prior to and at limb contact have been shown to play crucial roles in slip severity (Moyer et al., 2006). A limb usually begins to slide once contact is made with a low-friction surface and the sliding distance, or slip displacement, is proposed to dictate the probability of a fall. For humans walking on slippery ground, the minimum slip distance threshold to induce falling is proposed to be 10 cm (Strandberg and Lanshammar, 1981). The likelihood of falling is also known to increase when the limb contacts the ground at smaller angles (Brady et al., 2000). Furthermore, falls frequently result when the COM fails to cross over the BOS during limb–ground contact (You et al., 2001; Bhatt et al., 2006; Cappellini et al., 2010). Given the tolerance of mass-spring systems for considerable variations in limb stiffness and limb contact angle at higher running speeds (Seyfarth et al., 2002), a body moving at higher speeds could be less sensitive to perturbations such as low-friction terrain (see Daley and Biewener, 2006). Higher speed at limb contact is thought to play a role in the trajectory of the COM during the stance phase, as it is known that faster velocities of the COM relative to the BOS are integral to regaining balance when negotiating slippery terrain (You et al., 2001). However, it is not known whether these are common features of locomotion among terrestrial animals or common across different locomotor speeds.

In the present study, we used the helmeted guinea fowl as a model system for addressing the following questions: (1) what causes a fall when running over slippery surfaces; (2) is there a minimum slip distance threshold to induce falling, as suggested by Strandberg and Lanshammar (Strandberg and Lanshammar, 1981); (3) how can falls be averted when encountering slippery surfaces; and (4) do specific running speeds increase the propensity of fall avoidance or falling? We used high-speed video, kinetics and inverse dynamics approaches to investigate the biomechanics of traversing slippery and non-slippery surfaces. Specifically, we studied hindlimb function during stance phases on surfaces covered with sandpaper (non-slippery surface) and polypropylene (slippery surface). We hypothesized that fall avoidance over slippery terrain would be achieved with faster running speeds, which can induce faster COM velocities at limb contact and thus increase the likelihood of the COM passing over the BOS for successful completion of the stance phase. Larger limb contact angles and larger magnitudes of ground reaction force (GRF) were expected to facilitate fall avoidance. To avoid falls, the GRF must be large enough to support the body weight during limb–ground contact. Small GRF magnitudes would fail to support body weight and, depending on their magnitude and orientation, would limit the moments produced at joints. Because slip distances are associated with falls, we predicted that a slip distance threshold would be observed in guinea fowl.

MATERIALS AND METHODS

Animals

Four helmeted guinea fowl (*Numida meleagris* Linnaeus 1758) were housed at the Charles Lee Morgan Poultry Center at Clemson University. All birds were 10–12 months old and weighed 1.26–1.80 kg (1.55±0.20 kg, mean ± s.e.m.). On the day of experiments, a bird was transported to the laboratory at Clemson University and was anesthetized with an intramuscular injection of ketamine and xylazine. While under anesthesia, primary feathers were clipped to prevent flying and the feathers on and near the left hindlimb were plucked to visualize limb segments. Joint centers of rotation were found *via* palpation and each joint was marked with black ink overlying a larger blotch of white ink. Following experiments, birds were killed *via* intravenous injection of sodium pentobarbital. Procedures were approved by Clemson University's Institutional Animal Care and Use Committee.

Experiments

Birds ran along a 6.0×0.4 m runway with 0.76 m tall wooden sidewalls. A 1.6 m×0.76 m×0.5 cm (length×height×thickness) Plexiglas® sidewall was used in the middle of the runway to permit lateral high-speed video recordings and a 1.6×0.76 m (length×height) wooden sidewall in the middle was painted black to provide a contrasting background. A force plate (model 9260AA, Kistler, Amherst, NY, USA) was positioned in the middle of the runway and ~1.0 cm below the runway's surface to isolate the force plate surface from limb contact. A 0.3 m×0.3 m×1.0 cm (length×height×thickness) piece of plywood was positioned over a 0.3×0.3 m portion of the force plate surface to isolate single limb contacts as the birds ran along the middle of the runway. We glued a 0.3×0.3 m 150-grit sandpaper surface over the top surface of the plywood positioned on the force plate to produce a non-slippery running surface. We glued a 0.6×0.3 m polypropylene shelving liner (Seville Classics Inc., Torrance, CA, USA) on another piece of plywood (0.3 m×0.3 m×1.0 cm, length×width×thickness) to produce a slippery surface. The additional 0.3 m length on the polypropylene surface prevented recoveries in the cases when birds slipped. The thickness of both sandpaper and polypropylene surfaces equaled the thickness of the lining covering the floor of the runway. Trials in which birds ran over sandpaper were called SP-run treatments (see supplementary material Movie 1), trials in which birds successfully ran over polypropylene without falling were called PP-run treatments (see supplementary material Movie 2) and trials in which birds slipped and fell on polypropylene were called PP-fall treatments (see supplementary material Movie 3).

At the beginning of each experiment, we trained each specimen to run along the track and over sandpaper surfaces. Once the specimen was acclimated to the track, we began recording the first five experimental trials on sandpaper. Subsequent trials were randomly assigned with sandpaper and polypropylene surfaces. To avoid potential cases of fatigue, specimens were given 10-min resting intervals between trials. Data were collected from at least eight trials per surface per individual. We excluded data in cases when a portion of the supporting talon (not the whole talon) contacted the force plate, as these awkward talon positions preclude accurate GRF recordings and thus correct calculations of joint moments. The same criterion for excluding data was used for PP-surfaces. Also, data from PP-run trials were excluded in cases when a bird fell after the next limb contact, though these occasions were rare. From all specimens, we analyzed 71 individual trials, which included 30 trials on sandpaper and 41 trials on polypropylene.

Video recordings and analyses

Left lateral views of guinea fowl running behavior on sandpaper and polypropylene surfaces were recorded with a high-speed video camera (Photron APX-RS, San Diego, CA, USA) at 500 Hz and synchronized with force plate recordings *via* an external trigger.

Markings on the middle toe, tarsometatarsophalangeal (TMP) joint, ankle joint and knee joint were digitized using a custom MATLAB routine (Hedrick, 2008). Because feathers obstructed views of the hip and synsacrum in three of the four birds, we used the connection between the left wing and body (wing–body connection) as a static point that was used for determining body speed, limb length and limb contact angle. The height and proximity of the wing–body connection approximated hip height and the COM, respectively (Fig. 1A). In lateral view, approximate COM locations in *N. meleagris* occur slightly ventral to the wing–body connections (see Daley et al., 2006). From digitized videos, we measured body speed during stance phases (SP-runs and PP-runs only), approaching body speed prior to limb contact (PP-falls only), limb contact angle (the acute angle between the wing–body connection, the toe and horizontal), normalized limb length at limb contact (distance between the toe and wing–body connection divided by total limb length; total limb length was the sum of limb segment lengths), knee angle, ankle angle and TMP angle (Fig. 1A). We used the middle toe for measuring slip distance, which was the distance that the toe traveled between the onset of slipping and the offset of slipping (PP-run and PP-fall trials only).

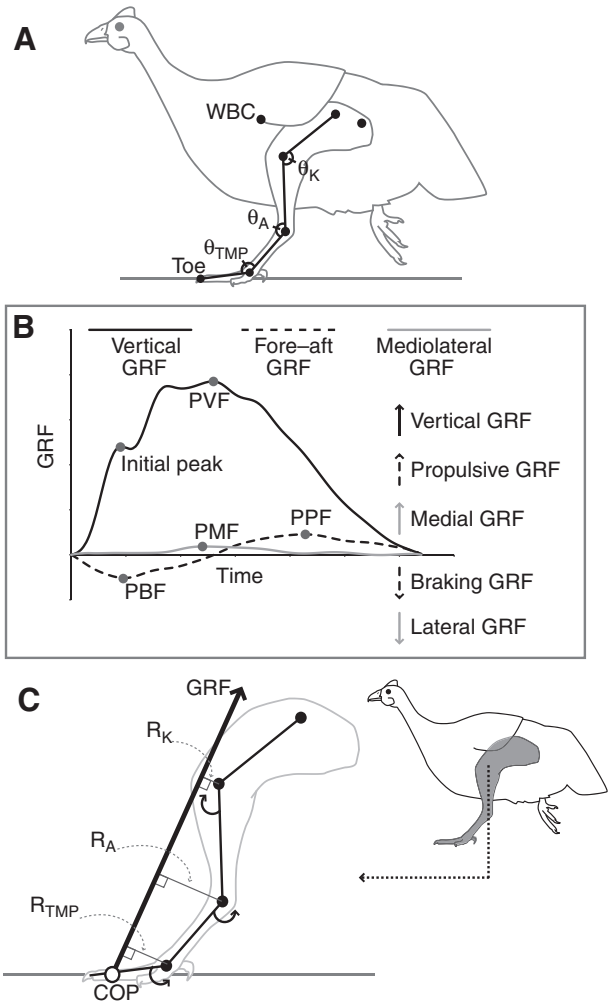

Fig. 1. Methods used for analyzing kinematics, kinetics and inverse dynamics data. (A) Coordinates used for calculating kinematics data. θ_A, ankle angle; θ_K, knee angle; θ_{TMP}, tarsometatarsophalangeal joint (TMP) angle; WBC, wing–body connection. (B) Ground reaction force (GRF) plotted in a reaction coordinate system and the criteria for measuring peak forces. Positive values for fore–aft and mediolateral forces represent propulsive and medial forces, respectively. Negative values for fore–aft and mediolateral forces represent braking and lateral forces, respectively. PBF, peak braking force; PMF, peak medial force; PPF, peak propulsive force; PVF, peak vertical force. (C) Schematic of variables used in calculating external joint moments using inverse dynamics approaches. Curved black arrows indicate the direction of positive moments produced at joints. COP, center of pressure (origin of GRF vector); R_A, ankle out-moment arm; R_K, knee out-moment arm; R_{TMP}, TMP out-moment arm.

Force recordings and analyses

The force platform was used to measure the vertical, fore–aft (braking–propulsive) and mediolateral components of the GRF, the two-dimensional orientation of the GRF and the center of pressure (COP). The directions of all GRF components were expressed in a reaction coordinate system with positive values for fore–aft and mediolateral forces representing propulsive and medial forces, respectively, and negative values for fore–aft and mediolateral forces represent braking and lateral forces, respectively (Fig. 1B). Amplified force signals were sampled at 1000 Hz and low-pass filtered with a 45 Hz cut-off frequency in AcqKnowledge 4.1 (Goleta, CA, USA). From filtered traces, we determined peak vertical GRF, peak braking GRF, peak medial GRF, vertical GRF load rate (change in vertical GRF between the onset of the vertical GRF to the initial peak divided by the respective change in time) and braking GRF load rate (change in braking GRF between the onset of braking GRF and the peak braking GRF divided by the respective change in time). GRF magnitudes were expressed in units of body weight (BW) and GRF loading rates were expressed in $BW\,s^{-1}$.

Inverse dynamics

Inverse dynamics approaches were used to calculate external moments at the knee, ankle and TMP joints (Fig. 1C). The joint moment is the product of GRF and the out-moment arm (R), which is the orthogonal distance from the GRF vector (the resultant vector from the vertical and fore–aft GRF components) to the joint's center of rotation (Biewener, 2003). By convention, extensor moments at each joint were positive. We did not include inertial components in our calculations for joint moments because the inertial and gravitational moments are expected to be negligible at distal joints and small at proximal joints in birds (Clark and Alexander, 1975).

Statistical analyses

If a dependent variable was significantly correlated with body speed, we first obtained the residuals from a least-squares regression in order to remove the effect of speed. These residuals were then used for subsequent analyses. We used non-transformed values of dependent variables that were independent of body speed. *T*-tests were performed to compare the means of the appropriate values of dependent variables between all treatments: SP-run, PP-run and PP-fall. Values for all variables are expressed as means ± s.e.m. The criterion for significance in all cases was $P<0.05$. However, to correct for multiple statistical tests, α was adjusted using a sequential Bonferroni test (Rice, 1989).

We included 13 variables in a principal components analysis (PCA) to reduce dimensionality and search for axes of correlated variation (Table 1). This approach transforms a large number of potentially correlated variables into a smaller number of uncorrelated variables (principal components). The purpose of the PCA was to determine the major axis of multivariate variation (PC1) that indicates which of the 13 variables (e.g. kinematics and kinetics) accounted for most of the variation in our data set. To verify that

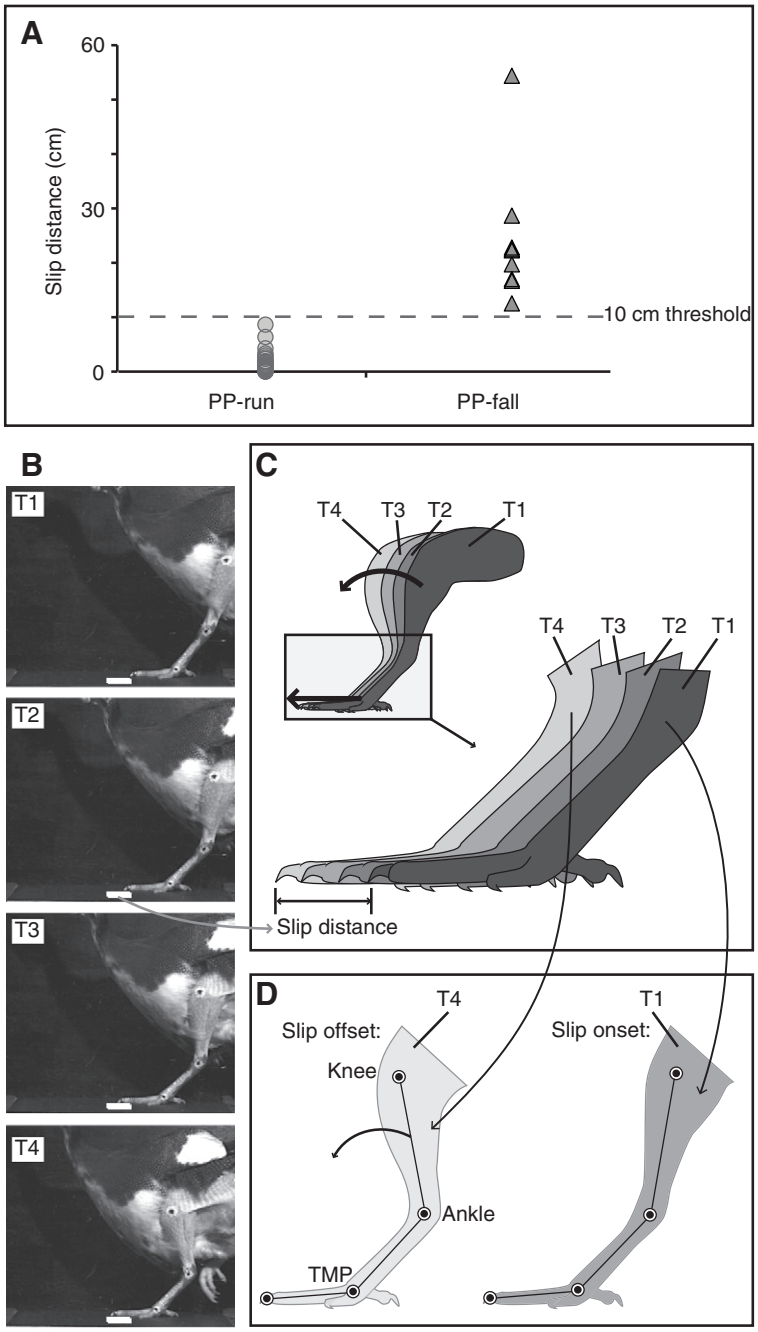

Fig. 2. Slip distance in helmeted guinea fowl running on low-friction polypropylene surfaces and the kinematic signals of slip cessation. (A) Slip distance in birds that avoided falling (PP-run) and birds that fell (PP-fall). Note that the previously proposed 10 cm slip-distance threshold for falls clearly demarcates the data from PP-run and PP-fall conditions. (B) Video images of the initial 18 ms of a stance phase on a polypropylene surface, which includes the onset of slipping (at T1) and the cessation of slipping (at T4). The interval between each video image is 6 ms. The small white line beneath the toe indicates the slip distance. (C) Schematic showing how slip distance was measured when a bird ran on a polypropylene surface. Slip distance was the distance covered by the tip of the middle toe between the onset of slipping (at T1) and the cessation of slipping (at T4). (D) Schematic showing the knee crossing over the ankle prior to the offset of slipping (at T4). In all cases when birds avoided falling (PP-run), the knee crossed over the ankle and slipping ceased when the knee was anterior to the ankle and posterior to the TMP joint.

experimental treatments occupied different regions in graphical space, we performed a two-way ANOVA with experimental treatments and individuals as independent variables and the scores from PC1 as the dependent variable.

RESULTS

Kinematics

Guinea fowl specimens fell in 22% of the trials occurring on polypropylene surfaces. During the initial 36 ms of the stance phase, limb contact angles always increased to a peak angle (60–82 deg) and then decreased during the fall. In cases when specimens did not fall (all PP-run and SP-run treatments), limb contact angles progressively increased during the stance phase. During the course of limb contact prior to falling, the knee and wing–body connection (the approximate COM) never crossed over the ankle or TMP joint. We used the TMP joint as an index for the BOS, which is analogous to using the human heel as a reference for BOS (You et al., 2001; Bhatt et al., 2006). Slipping began at limb contact with polypropylene surfaces, and mean slip distances were 1.5 and 20 cm in PP-run and PP-fall treatments, respectively (Fig. 2A). In PP-run treatments, 12% of the slip distances were less than 1 mm and 9% were greater than 4 cm, with the maximum slip distance at 8.6 cm. Slipping normally stopped when the knee crossed over the ankle (with the x-coordinate of the knee occurring between the x-coordinates of the ankle and TMP joint) (Fig. 2B–D).

Individuals ran over slippery and non-slippery surfaces at highly variable speeds ranging from 1.3 to 3.6 m s^{-1}, with SP-run and PP-run treatments reaching maximum speeds exceeding 3.5 m s^{-1} whereas the maximum speed in PP-fall treatments was 2.8 m s^{-1}. The mean speed in PP-run treatments was significantly greater than

Table 1. Loadings from principal components analysis of kinematics and kinetics variables measured in helmeted guinea fowl

Variable	PC1	PC2
Body speed	0.537	–0.180
Normalized limb length at limb contact	**0.858**	0.239
Limb contact angle	**0.789**	–0.369
TMP angle at limb contact	**–0.807**	0.395
Ankle angle at limb contact	–0.474	–0.011
Peak vertical GRF	**0.794**	0.561
Vertical GRF load rate	0.305	**0.735**
Peak braking GRF	–0.020	–0.555
Braking GRF load rate	0.134	**0.872**
Peak propulsive GRF	**0.683**	–0.390
Peak medial GRF	**0.670**	–0.362
Peak ankle extensor moment	–0.185	**0.734**
Peak TMP extensor moment	0.463	**0.742**

PC1 and PC2 explained 34.1 and 28.3% of the total variance, respectively.
GRF, ground reaction force; TMP, tarsometatarsophalangeal joint.
Loadings with a magnitude greater than 0.6 and less than –0.6 are marked in bold.

mean approach speed in PP-fall treatments (*t*-test, $P<0.05$). Despite the substantial variation in body speed, the kinematic variables we analyzed (limb contact angle, normalized limb length at limb contact, slip distance, knee angle, ankle angle and TMP joint angle) were independent of speed (Fig. 3).

Limb contact angle was significantly lower in PP-fall treatments than in SP-run (*t*-test, $P<0.001$) and PP-run treatments (*t*-test, $P<0.001$). Mean limb contact angles in both SP-run and PP-run treatments were 80 deg, with most limb contact angles falling between 80 and 90 deg (Fig. 3B, Fig. 4; Table 2). In PP-falls, mean limb contact angles were 66±1.82 deg and barely exceeded 70 deg in two of nine cases (Fig. 3B, Fig. 4, Table 2). PP-fall treatments comprised shorter limb lengths and larger TMP angles at limb contact than SP-run treatments (*t*-tests, $P<0.05$ and $P<0.001$, respectively) and PP-run treatments (*t*-tests, $P<0.01$ and $P<0.001$, respectively) (Table 2). Though there is no apparent relationship between speed and limb contact angle (Fig. 3B), it is clear that falls only occurred in a critical zone involving the combination of speeds less than 2.8 m s^{-1} and limb contact angles less than 72 deg (Fig. 4).

Lower limb length and larger TMP angle at limb contact were concomitant with the smaller limb contact angles for trials in which birds fell on slippery surfaces (Fig. 5). Birds occasionally ran over sandpaper while using a combination of large TMP angle or short limb length with small limb contact angle; however, these combinations were rarely used by birds that successfully ran over the slippery surface. Seventy-five percent of encounters on polypropylene surfaces involving the combination of large TMP angles (>142 deg) or short normalized limb lengths (<0.63) with small limb contact angles (<72 deg) resulted in a fall (Fig. 5). These kinematic combinations also demonstrate critical zones where falls were typically unavoidable during encounters with slippery surfaces. The long slip distances associated with falls normally resulted when birds contacted slippery surfaces with a small limb angle (<72 deg) and a large TMP angle (>142 deg) (Fig. 6). On fewer occasions were the combinations of small limb contact angles and large TMP angles at contact with polypropylene surfaces associated with short slip distances and fall avoidance. Knee and ankle angles at limb contact were similar in all treatments. Knee angles in PP-fall treatments were comparable to those in SP-run (*t*-test, $P=0.76$) and PP-run treatments (*t*-test, $P=0.84$), and ankle angles in PP-fall treatments were comparable to those in SP-run (*t*-test, $P=0.21$) and PP-run

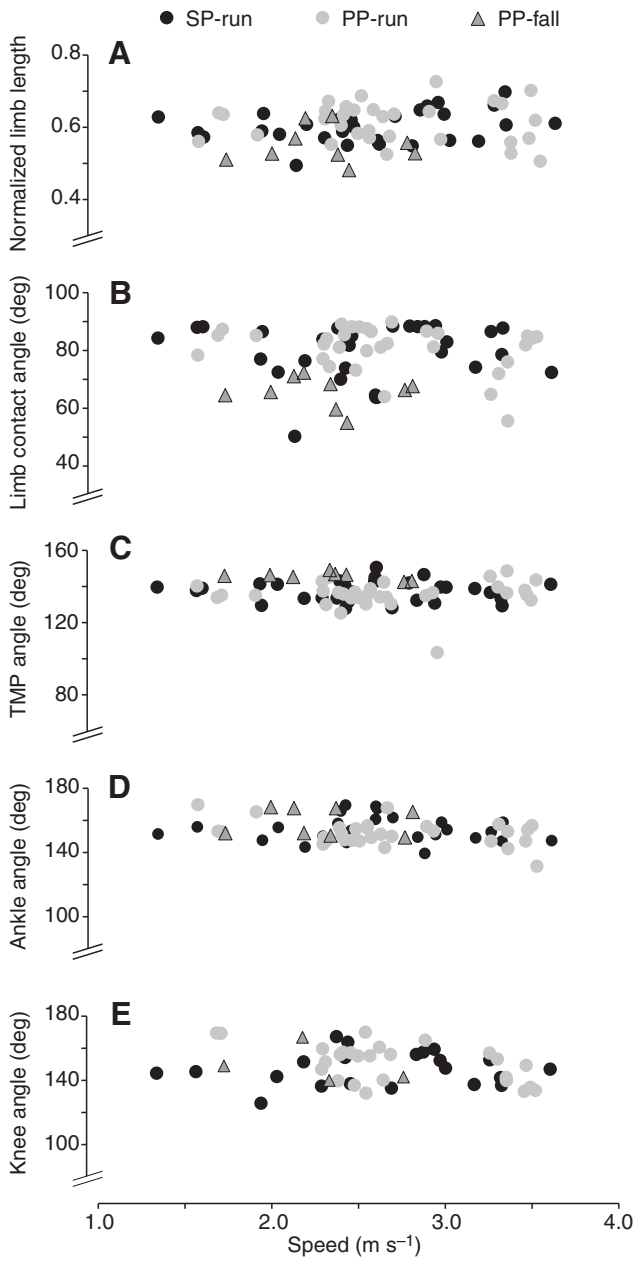

Fig. 3. Scatter plots of kinematic variables relative to running speed for SP-run, PP-run and PP-fall treatments. Note that all kinematic variables were independent of running speed. The plots show the relationship between body speed and (A) normalized limb length, (B) limb contact angle, (C) TMP angle, (D) ankle angle and (E) knee angle.

treatments (*t*-test, $P=0.064$). Following limb contact, birds in the SP-run and PP-run treatments exhibited nearly identical joint angle profiles during the stance phase (Fig. 7A). In contrast to these joint angle traces, there was minimal fluctuation in the joint angles prior to falling.

Ground reaction forces

We compared the residuals of all GRF variables, as they correlated with body speed. In sandpaper trials, a peak vertical GRF occurred during the initial 15–25% of stance and a larger peak occurred at approximately mid-stance. These vertical loading patterns were also

Table 2. Mean values of kinematics, kinetics and inverse dynamics variables measured in helmeted guinea fowl in all three experimental treatments (SP-run, PP-run and PP-fall)

Variable	SP-run	PP-run	PP-fall
Body speed (m s^{-1})	2.53±0.10	2.64±0.10	2.30±0.13
Limb contact angle (deg)	79.5±1.77	80.9±1.40	65.6±1.82
Normalized limb length at limb contact	0.60±0.010	0.61±0.010	0.55±0.017
Knee angle at limb contact (deg)	147.3±2.30	150.9±2.32	149.5±6.10
Ankle angle at limb contact (deg)	154.5±1.54	152.1±1.38	159.1±3.09
TMP angle at limb contact (deg)	137.5±1.08	135.7±1.36	145.7±0.75
Peak vertical GRF (BW)	2.38±0.083	2.37±0.084	1.53±0.20
Peak braking GRF (BW)	–0.635±0.044	–0.675±0.027	–0.633±0.089
Peak propulsive GRF (BW)	0.160±0.017	0.190±0.018	N/A
Peak medial GRF (BW)	0.0192±0.27	0.0308±0.40	0.00953±0.023
Vertical GRF load rate (BW s^{-1})	82.4±6.27	68.3±5.05	52.8±8.61
Braking GRF load rate (BW s^{-1})	–23.3±2.05	–20.5±1.17	–18.6±3.20
Peak knee extensor moment (Nm)	0.345±0.025	0.470±0.067	N/A
Peak knee flexor moment (Nm)	–1.64±0.11	–1.52±0.14	–1.83±0.091
Peak ankle extensor moment (Nm)	2.87±0.12	2.60±0.14	2.28±0.32
Peak TMP extensor moment (Nm)	1.93±0.087	1.80±0.10	1.29±0.17

Values are means ± s.e.m.
GRF, ground reaction force; N/A, not applicable; TMP, tarsometatarsophalangeal joint.

observed in some of the cases when birds successfully traversed polypropylene surfaces, though in most cases the initial peak was either absent or minimal (Fig. 7B). Thus, vertical loading rates were higher on sandpaper than on polypropylene surfaces (Table 2). Vertical loading rates were similar in both PP-run and PP-fall treatments (*t*-test, P=0.82). Despite differential vertical GRF traces and vertical loading rates, mean peak vertical loads were similar in both SP-run and PP-run treatments (*t*-test, P=0.41) (Fig. 7B, Table 2), and were significantly greater than the mean peak vertical loads in PP-fall treatments (*t*-tests, P<0.01). In the cases where birds fell on polypropylene surfaces, peak vertical GRFs were attained at peak limb contact angles. Peak braking GRFs and braking load rates were similar in all treatments. Peak propulsive GRFs were similar in both SP-run and PP-run treatments (*t*-test, P=0.48); however, propulsive GRFs were absent in all PP-fall treatments. Birds experienced a large range of peak medial GRFs on polypropylene surfaces, with the greatest forces occurring in PP-run treatments and the smallest forces in PP-fall treatments.

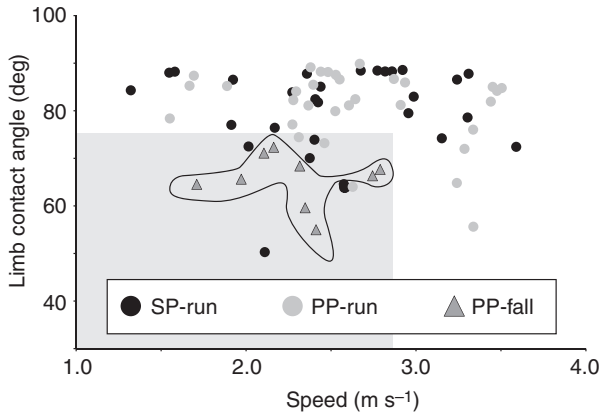

Fig. 4. Limb contact angles in helmeted guinea fowl from all three treatments plotted relative to body speed. PP-fall treatments were highlighted to show the significantly small limb contact angles, which were rarely attained by birds in SP-run and PP-run treatments. The shaded region represents a critical zone, where falls were typically unavoidable during encounters with slippery surfaces. This zone was bound within speeds less than 2.8 m s^{-1} and limb contact angles less than 72 deg.

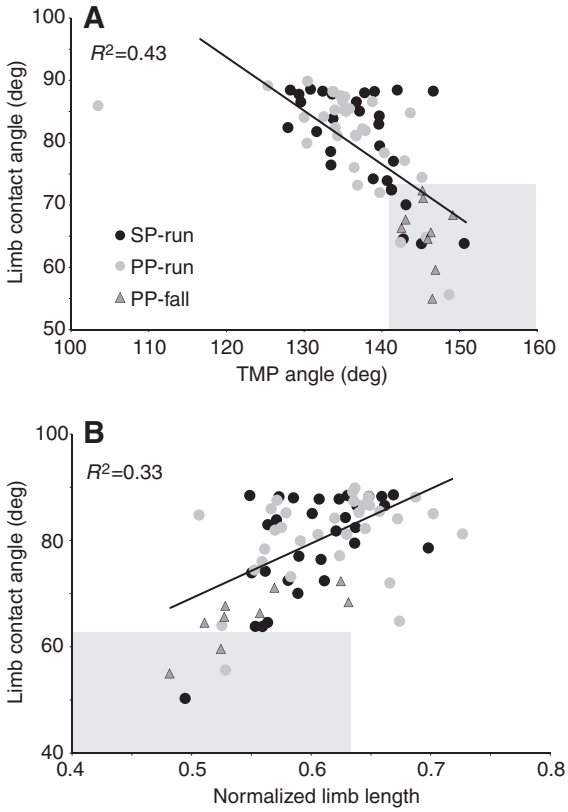

Fig. 5. Plots of limb contact angle in helmeted guinea fowl relative to TMP angle and normalized limb length. (A) Relationship between limb contact angle and TMP angle in SP-run, PP-run and PP-fall treatments. The critical zone (shaded area) was bound within large TMP angles (>142 deg) and small limb contact angles (<72 deg). (B) Relationship between limb contact angle and normalized limb length in all three treatments. The critical zone was bound within short limb lengths (<0.63) and small limb contact angles (<72 deg).

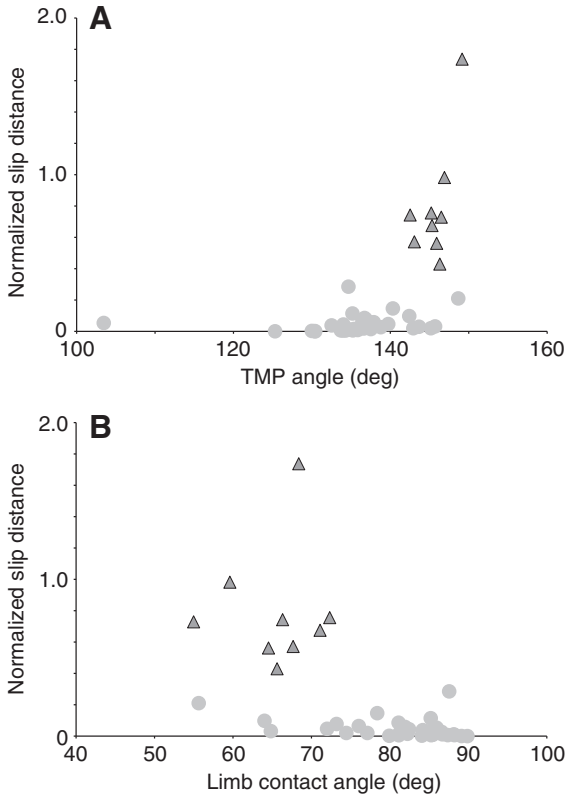

Fig. 6. Plots of normalized slip distance in helmeted guinea fowl relative to TMP angle and limb contact angle. Normalized slip distance was the distance that the middle toe traveled between the onset of slipping and the offset of slipping (PP-run and PP-fall trials only) divided by total limb length (total limb length equaled the sum of limb segment lengths). Both relationships show a clear separation of PP-fall and PP-run treatments. (A) Relationship between slip distance and TMP angle. TMP angles greater than 142 deg usually preceded the long slip distances that resulted in falls. (B) Relationship between slip distance and limb contact angle. Limb contact angles less than 72 deg were normally associated with the long slip distances that preceded falls.

Joint moments

In all conditions, the largest peak moments were recorded at the ankle, followed by the TMP and knee joints (Fig. 7C, Table 2). Positive (extensor) moments were produced at both the ankle and TMP joints throughout the duration of the stance and peaked at 40–50% of the stance (Fig. 7C). In SP-run and PP-run treatments, moments at the knee shifted from negative (flexor) during the initial half of the stance to positive (extensor) during the second half of the stance (Fig. 7C). Extensor moments at the knee were absent during falls (Fig. 7C). Extensor moments at the ankle and TMP were similar in all treatments. Peak ankle extensor moments in PP-fall treatments were comparable to those in SP-run (*t*-test, P=0.88) and PP-run treatments (*t*-test, P=0.46). Also, peak TMP extensor moments in PP-fall treatments were comparable to those in SP-run (*t*-test, P=0.060) and PP-run treatments (*t*-test, P=0.40). Peak extensor moments at the knee were similar in SP-run and PP-run treatments (*t*-test, P=0.11).

Principal components analysis

The percent of variation in kinematics, kinetics and inverse dynamics explained by the first two principal components was 34.1 and 28.3%, respectively (Table 1). Variables that loaded strongly on PC1 (absolute value of loadings greater than 0.6) were normalized limb length, limb contact angle, TMP angle at limb contact, peak vertical GRF, peak propulsive GRF and peak medial GRF (Table 1, Fig. 8). Vertical GRF loading rate, braking GRF loading rate, peak ankle extensor moment and peak TMP extensor moment loaded strongly on PC2 (Table 1, Fig. 8). From the two-way ANOVA, in which we compared PC1 scores between treatments and individuals, we found that PP-fall treatments differed significantly from SP-run and PP-run treatments with respect to normalized limb length, limb contact angle, TMP angle, peak vertical GRF, peak propulsive GRF and peak medial GRF (P=0.019); however, individual effects were weak (P=0.377). There were no differences between treatments on PC2.

DISCUSSION

Small limb angle, short limb length and large TMP joint angle at limb contact are kinematic parameters that cause falls on low-friction surfaces. The increased TMP angles in *N. meleagris* parallel the increased knee and ankle joint angles that cause humans to lose balance on slippery surfaces (Cham and Redfern, 2001), and are associated with the highly acute limb contact angles that preceded falls. Limb contact angle, limb length and TMP angle were kinematic variables with the strongest loadings on PC1 (Fig. 8, Table 1). Large TMP angles and short limb lengths were related to small limb angles (Fig. 5). The limb contact angle threshold we observed for falling was 72 deg (Figs 3, 5, 6). Falls were imminent when guinea fowl ran on slippery surfaces with limb contact angles less than 72 deg, TMP angles greater than 142 deg and normalized limb lengths less than 0.63 (Fig. 5). Limb contact angle is a significant kinematic variable in avoiding falls when encountering slippery surfaces and other types of perturbations. Daley and Biewener found that increased limb contact angles in *N. meleagris* decreased GRF impulse magnitudes after experiencing unexpected drops in terrain height (Daley and Biewener, 2006). Humans also implement higher limb contact angles and shorter stride lengths for avoiding falls on slippery surfaces (Brady et al., 2000; You et al., 2001); however, decreased limb contact angles have been observed when slippery conditions were anticipated (Cham and Redfern, 2002b; Chambers et al., 2003).

Low running speeds on low-friction surfaces do not necessarily cause falls, as the running speeds of birds that fell (1.7–2.8 m s^{-1}) occurred within the range of running speeds of birds that successfully traversed slippery surfaces (1.5–3.5 m s^{-1}). Even though a combination of running speeds less than 2.8 m s^{-1} and limb contact angles less than 72 deg also comprised a critical zone for falls, speeds exceeding 3.0 m s^{-1} facilitated fall avoidance, even with limb contact angles below 70 deg (Fig. 3B, Fig. 4). Therefore, high running speeds permitted a larger variation in limb contact angle, whereas only high limb contact angles allowed fall avoidance at speeds below 3.0 m s^{-1} (Fig. 3B, Fig. 4). These results corroborate those from Seyfarth et al. (Seyfarth et al., 2002), in that mass-spring systems moving at higher speeds tolerate large variations in limb contact angle and limb stiffness, and thus are less sensitive to perturbations. Considering the decreased sensitivity associated with increased running speed, it is unlikely that small limb contact angles would precede falls on slippery terrain speeds exceeding the maxima we observed. Also, human walking speed has been shown to be strongly correlated with stability against balance loss at the onset of slipping (Bhatt et al., 2005).

Contacting the ground with greater limb angles and smaller TMP angles permits the proximal joints (knee and hip) and the COM to cross over the body's BOS (represented by the TMP joint), which is imperative for initiating limb lift-off at the end of the stance phase.

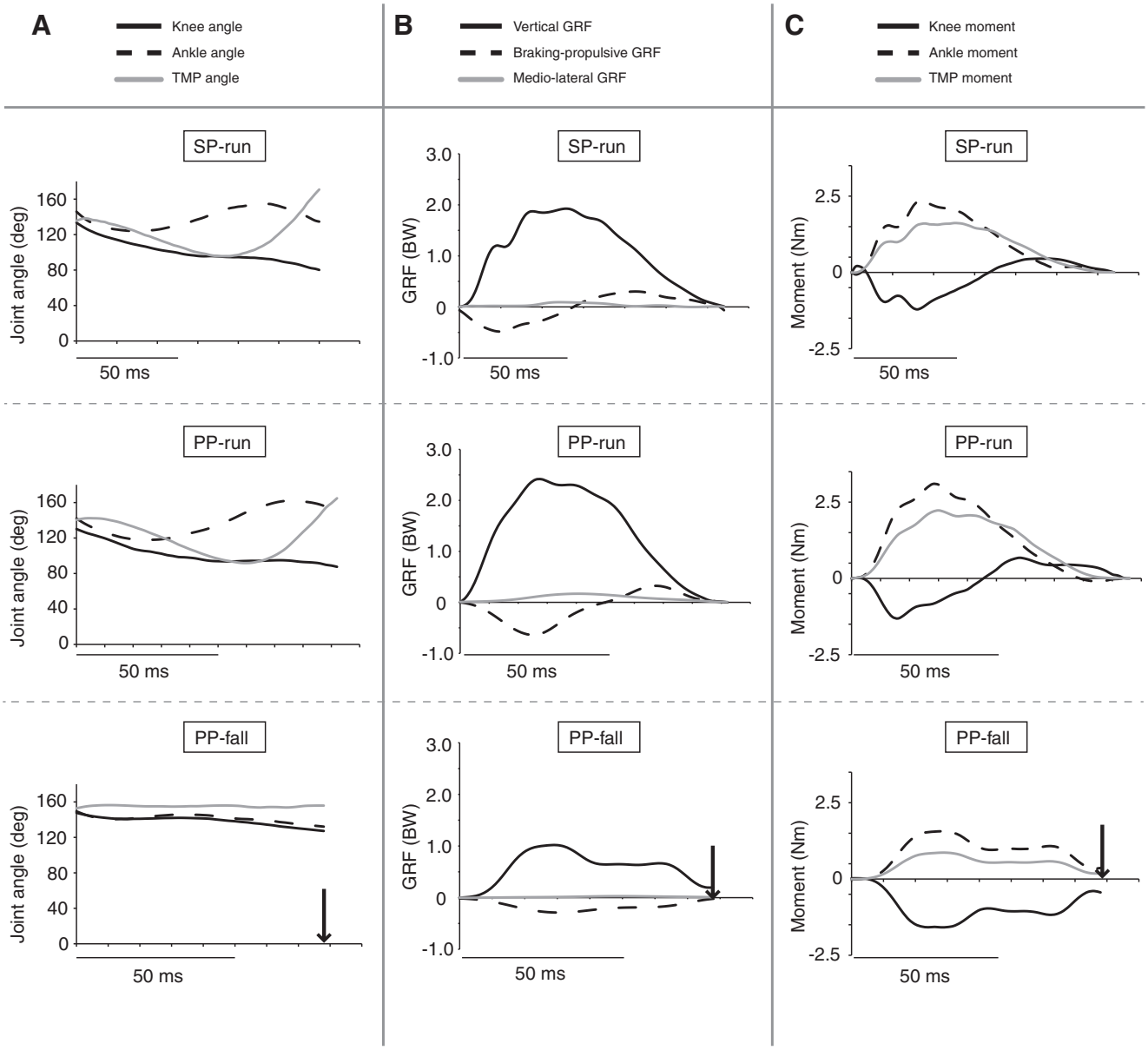

Fig. 7. (A) Joint angle, (B) GRF and (C) joint moment traces from SP-run, PP-run and PP-fall treatments. These data are representative of one individual helmeted guinea fowl specimen. Arrows indicate when the left limb slid off of the force plate surface in the PP-fall treatment.

An anterior shift in the COM over the supporting limb increases stability and the propensity for fall avoidance on slippery surfaces (You et al., 2001; Bhatt et al., 2006; Cappellini et al., 2010). Slipping in *N. meleagris* ceased once the knee crossed over the ankle (Fig. 2B–D), and short slip distances (<10 cm) typically resulted when the limb contacted the ground with larger limb angles and smaller TMP angles (Fig. 6). Specimens that fell experienced significantly smaller peak vertical and medial GRFs. Smaller GRFs can be expected in cases when the COM fails to pass over the BOS. Extensor moments did not occur at the knee joints of specimens that fell. Though small in relation to the peak extensor moments produced at the ankle and TMP, which were similar in all treatments, knee extensor moments are also required for limb retraction and thus facilitate successful completion of a stance phase. Specifically, the knee extensor moment counterbalances the GRF vector oriented posterior to the center of rotation of the knee during limb retraction, which comprises the latter half of the stance phase. Because the GRF vectors remained anterior to the knee center of rotation during the stance phases preceding falls, extensor moments were absent.

The absolute slip distance threshold we observed in *N. meleagris* across variable speeds was 10 cm, which agrees with the previously proposed and experimentally verified 10 cm slip distance threshold in walking humans (Strandberg and Lanshammar, 1981; Perkins and Wilson, 1983; Strandberg, 1983; Cham and Redfern, 2002a; Chambers et al., 2003) (but see Brady et al., 2000). The maximum slip distance in cases when birds avoided falling was 8.6 cm and the minimum slip distance when birds fell was 13 cm (Fig. 2). In addition to contacting the ground with larger limb angles and smaller TMP angles, the underlying significance of this threshold is likely the COM displacement relative to the body's BOS. You et al. found that greater forward COM velocities relative to the BOS are needed to avoid falling on low-friction surfaces (You et al., 2001). If the

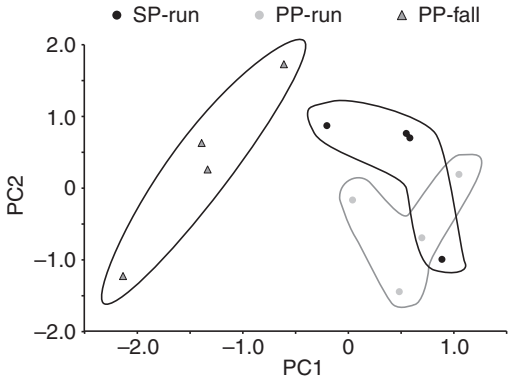

Fig. 8. Results (factor scores) from a principal components analysis using 10 variables from SP-run, PP-run and PP-fall treatments. Each factor score represents each combination for an individual and a treatment. Error bars are excluded because the factor scores were derived from mean values of each variable. The 10 variables plotted had loadings that were greater than 0.6 or less than –0.6. Note that the variables from PP-fall treatments differed significantly from SP-run and PP-run treatments with respect to PC1 but not PC2. PC1 variables: vertical load rate, braking load rate, peak ankle extensor moment and peak TMP extensor moment. PC2 variables: height, limb contact angle, TMP angle, peak vertical GRF, peak propulsive GRF and peak medial GRF.

BOS covers a large enough distance or reaches higher forward velocities than the COM while sliding on a slippery surface, the COM will trail behind the BOS, fail to cross over the BOS and falling will result. In cases when *N. meleagris* avoided falling on polypropylene surfaces, slipping ceased once the COM crossed over the BOS.

Although we collected data from birds that ran at speeds ranging from 1.3 to 3.6 m s^{-1}, limb contact angle, normalized limb length at limb contact, slip distance and knee, ankle and TMP angles (at limb contact) were independent of speed (Fig. 3). This is a surprising result because speed is known to have important effects on kinematics (Fieler and Jayne, 1998; Gatesy, 1999) and muscle function (Roberts et al., 1997; Daley and Biewener, 2003; Higham et al., 2008). However, in a previous study, guinea fowl conserved their limb contact angles across an even larger range in speed (0.2–4.17 m s^{-1}) (Gatesy, 1999). Furthermore, conserved limb contact patterns across various speeds are known in a variety of galliforms, ratites and other avian bipeds (Gatesy and Biewener, 1991; Gatesy, 1999). In addition to independence from body speed, mean limb contact angles in the present study were conserved across different substrates in cases when falls were avoided (Table 2).

The present study represents an exploratory approach to investigating how helmeted guinea fowl avoid falling on slippery surfaces. There are, however, some limitations with our study. We recorded and analyzed data from the stance phases of single limb contacts, instead of whole strides and multiple limb contacts. Though we did not study multiple limb contacts, guinea fowl avoided falling on the second limb contact in more than 95% of successful encounters with low-friction surfaces (PP-runs) (A.J.C. and T.E.H., unpublished). Data from stance phases (PP-run only) preceding falls during the second step were excluded from this study. Even though recordings of whole strides and multiple limb contacts provide a more extensive view of the COM trajectory, the COM motion relative to the BOS during limb contact with a low-friction surface is crucial to losing or restoring dynamic stability. Dynamic stability plays a significant role in fall avoidance among large animals (birds and mammals) and even smaller hexapedal animals (Ting et al., 1994; Full et al., 2002). When the supporting limb contacts the ground, the COM must pass over the BOS in order to achieve dynamic stability (You et al., 2001). During stance phases on polypropylene, helmeted guinea fowl achieved dynamic stability if the COM passed over the BOS, which kept slip distances (BOS displacement) minimal and thus produced a secure foothold necessary for limb retraction.

CONCLUSIONS

Helmeted guinea fowl retained adequate limb control for the majority of encounters with low-friction surfaces at variable running speeds. Our results show that locomotor characteristics prior to and at limb contact on a low-friction surface dictate the propensity for falling. Contacting the ground with limb angles below 70 deg at running speeds less than 3.0 m s^{-1} induced a cascade of interrelated events that resulted in a fall: failure of the COM to cross over the BOS, insufficient vertical GRFs and the absence of knee extensor moments and propulsive GRFs; all of which occurred over a slip distance exceeding 10 cm. Falls were circumvented when approaching slippery surfaces at higher running speeds and larger limb contact angles, which allow the COM to pass over the BOS, restrict slip distances and maximize vertical GRFs, thus facilitating limb retraction and the conclusion of the stance phase. Our study demonstrates common limb control strategies on slippery surfaces in helmeted guinea fowl and humans, and therefore highlights the utility of guinea fowl as a model system for studying the mechanisms and dynamics of falling in humans. Future work assessing the neuromuscular control of the limb during slipping would further enhance our understanding of fall avoidance and potentially contribute to the development of stable robots (Renner and Behnke, 2006).

LIST OF ABBREVIATIONS

BOS	base of support
BW	body weight
COM	center of mass
COP	center of pressure
GRF	ground reaction force
PBF	peak braking force
PCA	principal components analysis
PMF	peak medial force
PP	polypropylene
PPF	peak propulsive force
PVF	peak vertical force
R	out-moment arm
SP	sandpaper
TMP	tarsometatarsophalangeal joint
WBC	wing–body connection

ACKNOWLEDGEMENTS

We thank Rick Blob for his advice on the experimental set-up and data analysis, Emily Kane for assisting with some experiments and Carol Foster-Mosley (Morgan Poultry Center) for animal care. Comments from two anonymous reviewers significantly improved an earlier version of this manuscript. Start-up funds from Clemson University (to T.E.H.) provided support.

REFERENCES

Biewener, A. A. (2003). *Animal Locomotion.* New York: Oxford University Press.
Biewener, A. A. and Daley, M. A. (2007). Unsteady locomotion: integrating muscle function with whole body dynamics and neuromuscular control. *J. Exp. Biol.* **210**, 2949-2960.
Biewener, A. A. and Gillis, G. B. (1999). Dynamics of muscle function during locomotion: accommodating variable conditions. *J. Exp. Biol.* **202**, 3387-3396.
Bhatt, T., Wening, J. D. and Pai, Y.-C. (2005). Influence of gait speed on stability: recovery from anterior slips and compensatory stepping. *Gait Posture* **21**, 146-156.
Bhatt, T., Wening, J. D. and Pai, Y.-C. (2006). Adaptive control of gait stability in reducing slip-related backward loss of balance. *Exp. Brain Res.* **170**, 61-73.

Brady, R. A., Pavol, M. J., Owings, T. M. and Grabiner, M. D. (2000). Foot displacement but not velocity predicts the outcome of a slip induced in young subjects while walking. *J. Biomech.* **33**, 803-808.
Cappellini, G., Ivanenko, Y. P., Dominici, N., Poppele, R. E. and Lacquaniti, F. (2010). Motor patterns during walking on a slippery walkway. *J. Neurophysiol.* **103**, 746-760.
Cavagna, G. A., Heglund, N. C. and Taylor, C. R. (1977). Mechanical work in terrestrial locomotion: two basic mechanisms for minimizing energy expenditure. *Am. J. Physiol. Regul. Integr. Comp. Physiol.* **233**, 243-261.
Cham, R. and Redfern, M. S. (2001). Lower extremity corrective reactions to slip events. *J. Biomech.* **34**, 1439-1445.
Cham, R. and Redfern, M. S. (2002a). Heel contact dynamics during slip events on level and inclined surfaces. *Safety Science* **40**, 559-576.
Cham, R. and Redfern, M. S. (2002b). Changes in gait when anticipating slippery floors. *Gait Posture* **15**, 159-171.
Chambers, A. J., Margerum, S., Redfern, M. S. and Cham, R. (2003). Kinematics of the foot during slips. *Occup. Ergon.* **3**, 225-234.
Clark, J. and Alexander, R. M. (1975). Mechanics of running by quail (*Coturnix*). *J. Zool. Lond.* **176**, 87-113.
Cooper, R. C., Prebeau-Menezes, L. M., Butcher, M. T. and Bertram, J. E. A. (2008). Step length and required friction in walking. *Gait Posture* **27**, 547-551.
Daley, M. A. and Biewener, A. A. (2003). Muscle force-length dynamics during level *versus* incline locomotion: a comparison of *in vivo* performance of two guinea fowl ankle extensors. *J. Exp. Biol.* **206**, 2941-2958.
Daley, M. A. and Biewener, A. A. (2006). Running over rough terrain reveals limb control for intrinsic stability. *Proc. Natl. Acad. Sci. USA* **103**, 15681-15686.
Daley, M. A., Usherwood, J. R., Felix, G. and Biewener, A. A. (2006). Running over rough terrain: guinea fowl maintain dynamic stability despite a large unexpected change in substrate height. *J. Exp. Biol.* **209**, 171-187.
Daley, M. A., Felix, G. and Biewener, A. A. (2007). Running stability is enhanced by a proximo-distal gradient in joint neuromechanical control. *J. Exp. Biol.* **210**, 383-394.
Ferris, D. P., Liang, K. and Farley, C. T. (1999). Runners adjust leg stiffness for their first step on a new running surface. *J. Biomech.* **32**, 787-794.
Fieler, C. I. and Jayne, B. C. (1998). Effects of speed on the hindlimb kinematics of the lizard *Dipsosaurus dorsalis*. *J. Exp. Biol.* **201**, 609-622.
Full, R. J., Kubow, T., Schmitt, J., Holmes, P. and Koditschek, D. (2002). Quantifying dynamic stability and maneuverability in legged locomotion. *Integr. Comp. Biol.* **42**, 149-157.
Gatesy, S. M. (1999). Guineafowl hind limb function. I: Cineradiographic analysis and speed effects. *J. Morphol.* **240**, 115-125.
Gatesy, S. M. and Biewener, A. A. (1991). Bipedal locomotion: effects of size, speed and limb posture in birds and humans. *J. Zool.* **224**, 127-147.
Hedrick, T. L. (2008). Software techniques for two- and three-dimensional kinematic measurements of biological and biomimetic systems. *Bioinspir. Biomim.* **3**, 034001.
Higham, T. E., Davenport, M. S. and Jayne, B. C. (2001). Maneuvering in an arboreal habitat: the effects of turning angle on the locomotion of three sympatric ecomorphs of *Anolis* lizards. *J. Exp. Biol.* **204,** 4141-4155.
Higham, T. E., Biewener, A. A. and Wakeling, J. M. (2008). Functional diversification within and between muscle synergists during locomotion. *Biol. Lett.* **4,** 41-44.
Jindrich, D. L. and Full, R. J. (2002). Dynamic stabilization of rapid hexapedal locomotion. *J. Exp. Biol.* **205**, 2803-2823.
Kannus, P., Parkkari, J., Niemi, S. and Palvanen, M. (2005). Fall-induced deaths among elderly people. *Am. J. Public Health* **95**, 422-424.
Kohlsdorf, T. and Biewener, A. A. (2006). Negotiating obstacles: running kinematics of the lizard *Sceloporus malachiticus*. *J. Zool.* **270**, 359-371.
Moyer, B. E., Chambers, A. J., Redfern, M. S. and Cham, R. (2006). Gait parameters as predictors of slip severity in young and older adults. *Erogonomics* **49**, 329-343.
Nishikawa, K., Biewener, A. A., Aerts, P., Ahn, A. N., Chiel, H. J., Daley, M. A., Daniel, T. L., Full, R. J., Hale, M. E., Hedrick, T. L. et al. (2007). Neuromechanics: an integrative approach for understanding motor control. *Integr. Comp. Biol.* **47**, 16-54.
Perkins, P. J. and Wilson, M. P. (1983). Slip resistance of testing shoes – new developments. *Ergonomics* **26**, 73-82.
Phillips, C. J. C. and Morris, I. D. (2001). The locomotion of dairy cows on floor surfaces with different frictional properties. *J. Dairy Sci.* **84**, 623-628.
Renner, R. and Behnke, S. (2006). Instability detection and fall avoidance for a humanoid using attitude sensors and reflexes. *Proc. IEEE/RSJ* **2006**, 2967-2973.
Rice, W. R. (1989). Analyzing tables of statistical tests. *Evolution* **43**, 223-225.
Roberts, T. J., Marsh, R. J., Weyland, P. G. and Taylor, C. R. (1997). Muscular force in running turkeys: the economy of minimizing work. *Science* **275**, 1113-1115.
Seyfarth, A., Geyer, H., Gunther, M. and Blickhan, R. (2002). A movement criterion for running. *J. Biomech.* **35**, 649-655.
Sponberg, S. and Full, R. J. (2008). Neuromechanical response of musculo-skeletal structures in cockroaches during rapid running on rough terrain. *J. Exp. Biol.* **211**, 433-446.
Strandberg, L. (1983). On accident analysis and slip-resistance measurement. *Ergonomics* **26**, 11-32.
Strandberg, L. and Lanshammar, H. (1981). The dynamics of slipping accidents. *J. Occup. Accid.* **3**, 153-162.
SWEA and Statistics Sweden (2000). *Occupational Diseases and Occupational Accidents 1998*. Stockholm: Swedish Work Environment Authority.
Thorup, V. M., Laursen, B. and Jensen, B. R. (2008). Net joint kinetics in the limbs of pigs walking on concrete floor in dry and contaminated conditions. *J. Anim. Sci.* **86**, 992-998.
Tinetti, M. E. and Williams, C. S. (1997). Falls, injuries due to falls, and the risk of admission to a nursing home. *N. Engl. J. Med.* **337**, 1279-1284.
Ting, L. H., Blickhan, R. and Full, R. J. (1994). Dynamic and static stability in hexapedal runners. *J. Exp. Biol.* **197**, 251-269.
US Bureau of Labor Statistics (1992). *Occupational Injury and Illness Classification Manual.* Washington, DC: US Government Printing Office.
You, J.-Y., Chou, Y.-L., Lin, C.-J. and Su, F.-C. (2001). Effect of slip on movement of body center of mass relative to base of support. *Clin. Biomech.* **16**, 167-173.